

Fluid-fluid demixing curves for colloid-polymer mixtures in a random colloidal matrix

Mario Alberto Annunziata

CNR, Istituto dei Sistemi Complessi

(Area della Ricerca di Roma Tor Vergata)

Via del Fosso del Cavaliere 100,

I-00133 Roma, Italy

and INFN, Sezione di Pisa

L.go Pontecorvo 3, I-56127 Pisa, Italy

e-mail: m.annunziata@isc.cnr.it

Andrea Pelissetto

Dipartimento di Fisica,

Università degli Studi di Roma “La Sapienza”

and INFN – Sezione di Roma I

Piazzale A. Moro 2,

I-00185 Roma, Italy

e-mail: Andrea.Pelissetto@roma1.infn.it

Abstract

We study fluid-fluid phase separation in a colloid-polymer mixture adsorbed in a colloidal porous matrix close to the θ point. For this purpose we consider the Asakura-Oosawa model in the presence of a quenched matrix of colloidal hard spheres. We study the dependence of the demixing curve on the parameters that characterize the quenched matrix, fixing the polymer-to-colloid size ratio to 0.8. We find that, to a large extent, demixing curves depend only on a single parameter f , which represents the volume fraction which is unavailable to the colloids. We perform Monte Carlo simulations for volume fractions f equal to 40% and 70%, finding that the binodal curves in the polymer and colloid packing-fraction plane have a small dependence on disorder. The critical point instead changes significantly: for instance, the colloid packing fraction at criticality increases with increasing f . Finally, we observe for some values of the parameters capillary condensation of the colloids: a bulk colloid-poor phase is in chemical equilibrium with a colloid-rich phase in the matrix.

PACS: 61.25.Hq, 82.35.Lr

I. INTRODUCTION

The study of the fluid phases in mixtures of colloids and nonadsorbing neutral polymers has become increasingly important in recent years; see Refs. [1–6] for recent reviews, Refs. [7–16] for experiments, and Refs. [17–40] for theoretical investigations. These systems show a very interesting phenomenology, which only depends to a large extent on the nature of the solvent and on the ratio $q \equiv R_g/R_c$, where R_g is the radius of gyration of the polymer and R_c is the radius of the colloid. Experiments and numerical simulations indicate that polymer-colloid mixtures have a solid colloidal phase for large enough colloidal concentrations and a corresponding fluid-solid coexistence. Much less obvious is the presence of a fluid-fluid coexistence of a colloid-rich, polymer-poor phase (colloid liquid) with a colloid-poor, polymer-rich phase (colloid gas). Extensive theoretical and experimental work indicates that such a transition occurs only if the size of the polymers is sufficiently large, i.e. for $q > q^*$, where [1, 26, 38] $q^* \approx 0.3-0.4$.

At least qualitatively, many aspects of the behavior of colloid-polymer suspensions can be understood by using the Asakura-Oosawa (AO) model [41, 42], which gives a coarse-grained description of the mixture. The polymers are treated as an ideal gas of point particles of radius R_p (which is usually identified with the radius of gyration) which interact with the colloids by means of a simple hard-core potential. This model is extremely crude since it ignores the polymeric structure and polymer-polymer repulsion, which is relevant in the good-solvent regime. Nonetheless, it correctly predicts polymer-colloid demixing as a result of the entropy-driven effective attraction (depletion interaction) between colloidal pairs due to the presence of the polymers [17–19, 21, 23–25, 31, 32]. It is not, however, quantitatively predictive for polymers in the good-solvent regime. For instance, at a given colloid packing fraction, the AO model predicts the binodal curve to be at a polymer volume fraction which is significantly lower than that observed experimentally. In order to reproduce the experimental results one can use realistic atomistic models for the polymers, but this is a very difficult task from a numerical point of view. In the colloid regime $q \lesssim 1$, it is much easier, and still provides good results, to use coarse-grained models in which polymers are modelled as point particles (as in the AO model) interacting with repulsive soft pair potentials [24, 26, 33, 40], which have either a phenomenological origin or are derived by means of exact coarse-graining procedures. Nonetheless, at least for $q \lesssim 1$ (colloidal regime), the AO model is expected

to provide quantitatively correct results for colloid-polymer solutions close to the θ point. Indeed, in this regime polymers show an approximate ideal behavior and can be described quite reasonably as noninteracting random walks, as does the AO model [43].

In this paper we wish to study the demixing of colloid-polymer mixtures in porous materials, which are characterized by a highly interconnected porous structure. They have important technological applications, for instance in catalysis and gas separation and purification [44]. Examples are the Vycor glasses, in which pore sizes range from 1 nm to 100 nm, and high-porosity systems like silica gels (xerogels and aerogels), which are produced by means of silica sol-gel processes. AO colloid-polymer mixtures in a porous matrix have been studied in Refs. [45–49] by means of density-functional theory, integral equations, and Monte Carlo (MC) simulations. The nature of the critical transition has been fully clarified [46–49]: if obstacles are random and there is a preferred affinity of the quenched obstacles to one of the phases, the transition is in the same universality class as that occurring in the random-field Ising model, in agreement with a general argument by de Gennes [50]. If these conditions are not satisfied, standard Ising or randomly dilute Ising behavior is observed instead, see Refs. [51, 52]. On the other hand, little is known on how demixing is influenced by the amount of disorder and by its nature (for a polymer matrix some results for the critical-point behavior as a function of the amount of disorder are reported in Ref. [46]). In this paper porosity is introduced by considering a quenched matrix of hard spheres of radius R_{dis} . We will compute the binodal curves in terms of the polymer and colloid packing fractions for different ratios R_{dis}/R_c and for different disorder concentrations with the purpose of determining how these parameters affect the location of the demixing transition and of the critical (second-order) transition point. We will not instead perform a detailed study of the q dependence and we shall set $q = 0.8$ as in Ref. [48]. This work complements the results of Ref. [45], which instead studied the q dependence for a single value of R_{dis}/R_c , $R_{\text{dis}}/R_c = 1$, and of the disorder concentration.

The paper is organized as follows. In Sec. II we discuss the model and the relevant variables. In Sec. III we present our numerical results. Our conclusions are presented in Sec. IV. In App. A we present some details on the MC calculation.

II. THE MODEL

In the AO model polymers and colloids are modelled as spheres of radii R_p and R_c , respectively. We assume hard-sphere interactions between colloid and colloid-polymer pairs; the pair potentials are given by

$$\begin{aligned}
 u_{cc}(r) &= \begin{cases} \infty & \text{for } r < 2R_c, \\ 0 & \text{for } r \geq 2R_c, \end{cases} \\
 u_{cp}(r) &= \begin{cases} \infty & \text{for } r < R_c + R_p, \\ 0 & \text{for } r \geq R_c + R_p, \end{cases} \\
 u_{pp}(r) &= 0,
 \end{aligned} \tag{1}$$

where r is the center-to-center distance. We consider a cubic box of size L and we characterize the thermodynamic phases in terms of the packing fractions

$$\eta_p \equiv \frac{4\pi R_p^3 N_p}{3L^3} \quad \eta_c \equiv \frac{4\pi R_c^3 N_c}{3L^3}, \tag{2}$$

where N_p and N_c indicate the number of polymers and of colloids in the box, respectively.

The phase behavior of the AO model has been extensively studied. It strongly depends on the polymer-to-colloid size ratio $q \equiv R_p/R_c$. For small values of q the demixing transition is unstable and only the fluid-solid transition occurs. Fluid-fluid demixing occurs [1, 26, 38] for $q \gtrsim 0.3-0.4$. In this work we have not investigated the q dependence of the binodal curve, since our main objective is the analysis of the role of quenched disorder. We have thus fixed $q = 0.8$, as in Ref. [48], at the boundary between the colloid and the protein regimes.

Disorder has been introduced by considering a colloidal quenched matrix which has a hard-sphere interaction both with the colloids and the polymers. In practice, we choose a disorder concentration c_{dis} and randomly distribute $N_{\text{dis}} = c_{\text{dis}}L^3$ nonoverlapping spheres of radius R_{dis} in the box. The position of these spheres is assumed to be fixed (quenched). Colloids and polymers can only move outside the quenched matrix, which means that the

spheres belonging to the matrix and the freely moving particles interact with pair potentials

$$\begin{aligned}
 u_{c,\text{dis}}(r) &= \begin{cases} \infty & \text{for } r < R_c + R_{\text{dis}}, \\ 0 & \text{for } r \geq R_c + R_{\text{dis}}, \end{cases} \\
 u_{p,\text{dis}}(r) &= \begin{cases} \infty & \text{for } r < R_p + R_{\text{dis}}, \\ 0 & \text{for } r \geq R_p + R_{\text{dis}}. \end{cases}
 \end{aligned} \tag{3}$$

Note that the matrices considered here are different from those discussed in Refs. [46, 47]. The main difference is that here the matrix consists in hard spheres that cannot intersect each other (we name it colloidal matrix). On the other hand, in Refs. [46, 47] the matrix spheres are soft and can freely overlap, as if they were an ideal gas (hence the name polymer matrix). Second, in those works, for a given choice of c_{dis} , the number N_{dis} is not fixed, but obtained from a Poissonian distribution with mean value $c_{\text{dis}}L^3$. This second difference should not be important in the infinite-volume limit, since it entails density fluctuations of order $1/L^{3/2}$, which vanish as $L \rightarrow \infty$.

In the simple model we consider, disorder is characterized by two parameters, the reduced concentration $\hat{c} \equiv c_{\text{dis}}R_c^3$ and the ratio R_{dis}/R_c . However, \hat{c} does not directly characterize the free space available to the colloids and to the polymers. We shall use instead the effective matrix filled-space ratio f , which is defined as follows. Consider the region \mathcal{R} in which the (centers of the) colloids are allowed:

$$\mathcal{R} = \{ \mathbf{r} : |\mathbf{r} - \mathbf{r}_i| \geq R_c + R_{\text{dis}}, \text{ for all } 1 \leq i \leq N_{\text{dis}} \}, \tag{4}$$

where \mathbf{r}_i is the position of the i -th hard sphere belonging to the matrix. If $V_{\mathcal{R}}$ is the volume of the region \mathcal{R} , we define

$$f \equiv 1 - \frac{[V_{\mathcal{R}}]}{L^3}, \tag{5}$$

where $[V_{\mathcal{R}}]$ is the average of $V_{\mathcal{R}}$ over the different matrix realizations. Note that, for large values of L , $[V_{\mathcal{R}}]$ is essentially independent of the matrix realization, a property known as self-averaging. The parameter f represents the volume fraction that is unavailable to the colloids due to the presence of the random matrix and can easily be determined by computing the probability of inserting a colloid in the otherwise empty matrix. In a completely analogous way we can define f_{pol} , which characterizes the volume fraction unavailable to polymers. Of

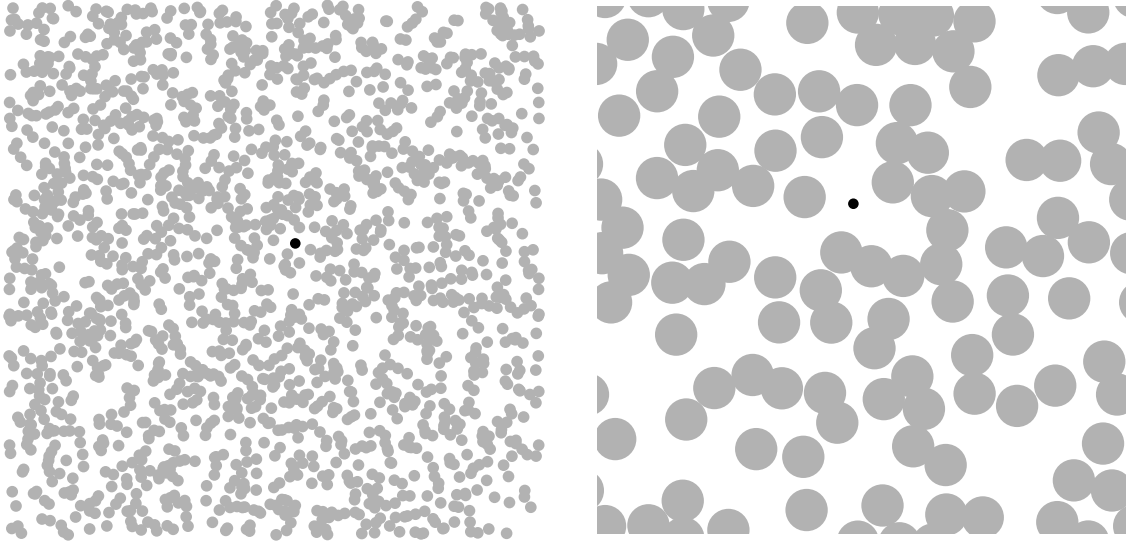


FIG. 1: Two-dimensional systems with $L/R_c = 50$ and $f = 0.5$. On the left we take $R_{\text{dis}}/R_c = 0.1$, while on the right $R_{\text{dis}}/R_c = 3.0$. The disorder packing fractions $\pi c R_{\text{dis}}^2$ are 0.0057 and 0.292 in the two cases, respectively. The gray circles of radius $R_c + R_{\text{dis}}$ correspond to the colloid-excluded region (depletion region) around each sphere of the quenched matrix: the centers of the colloids can only belong to the white region. We also draw a single colloid (black) to show the length scale.

course, $f > f_{\text{pol}}$ in the colloid regime in which $q < 1$, while $f < f_{\text{pol}}$ in the opposite, protein regime.

It is interesting to understand qualitatively how the disorder distribution changes with R_{dis} at fixed f . In Fig. 1 we show the matrix for $f = 0.5$ and two values of R_{dis} , $R_{\text{dis}}/R_c = 0.1$ and $R_{\text{dis}}/R_c = 3$. To make the figure more clear, we consider a two-dimensional system, that is a matrix of nonoverlapping disks on a square of area L^2 . It is evident that the topology of the matrix is quite different. For large R_{dis}/R_c the free volume available to the colloids consists in large empty regions connected by narrow channels. This is the case of a porous material with big interconnected pores. On the other hand, for R_{dis}/R_c small, pores are significantly smaller and the topology of the network is more complex.

In order to have demixing, the parameter f cannot be arbitrarily close to 1, but should satisfy $f < f^*$, where f^* is related to the percolation threshold of the region \mathcal{R} in which colloids can move. For $f > f^*$ the space \mathcal{R} divides in disconnected finite regions and thus no phase transition is possible. The exact value of f^* is unknown. However, the arguments

TABLE I: Estimates of the reduced concentration $\hat{c} \equiv c_{\text{dis}}R_c^3$ and of the disorder packing fraction $\eta_{\text{dis}} \equiv 4\pi R_{\text{dis}}^3 c_{\text{dis}}/3$ for two values of f and several values of R_{dis}/R_c .

R_{dis}/R_c	$f = 0.40$		$f = 0.70$	
	\hat{c}	η_{dis}	\hat{c}	η_{dis}
0.005	0.120	$6.3 \cdot 10^{-8}$	0.283	$1.5 \cdot 10^{-7}$
0.01	0.118	$4.9 \cdot 10^{-7}$	0.279	$1.2 \cdot 10^{-6}$
0.02	0.115	$3.9 \cdot 10^{-6}$	0.271	$9.1 \cdot 10^{-6}$
0.05	0.105	$5.5 \cdot 10^{-5}$	0.248	$1.3 \cdot 10^{-4}$
0.1	0.0915	$3.8 \cdot 10^{-4}$	0.215	$9.0 \cdot 10^{-4}$
0.2	0.0700	$2.3 \cdot 10^{-3}$	0.164	$5.5 \cdot 10^{-3}$
0.4	0.0431	0.0116	0.0972	0.026
0.6	0.0280	0.0254	0.0609	0.055
1.0	0.0136	0.057	0.0278	0.116

of Ref. [53] suggest

$$f^* \approx 0.85. \quad (6)$$

For the same reasons — polymers should be able to move in the whole space — the polymer parameter f_{pol} must satisfy $f_{\text{pol}} < f^*$ in order to observe coexistence.

In this paper we shall perform simulations for two values of f , $f = 0.40$ and $f = 0.70$, the latter being quite close to the threshold f^* , and for $q = 0.8$, so that $f_{\text{pol}} < f$. In Table I we report the reduced concentration \hat{c} and the disorder packing fraction $\eta_{\text{dis}} \equiv 4\pi R_{\text{dis}}^3 c/3$ for several values of R_{dis}/R_c . First, we observe that \hat{c} converges to a finite positive constant as $R_{\text{dis}}/R_c \rightarrow 0$. This result is quite easy to understand. If $R_{\text{dis}}/R_c \ll 1$, the pair potentials (3) become essentially independent of R_{dis} . Hence, the density becomes essentially independent of R_{dis} for R_{dis} small. In the opposite limit $R_{\text{dis}}/R_c \gg 1$, the potentials become essentially independent of R_c . Hence, in this limit f converges to the disorder packing fraction $\eta_{\text{dis}} \equiv 4\pi R_{\text{dis}}^3 c_{\text{dis}}/3$. For instance, for $\eta_{\text{dis}} = 0.30$, we obtain $f = 0.51, 0.40, 0.32$ for $R_{\text{dis}}/R_c = 5, 10, 50$. Since a liquid hard-sphere phase exists only up [54] to $\eta \approx 0.49$, for large R_{dis}/R_c , the matrix may belong to different hard-sphere phases, while still satisfying the condition $f < f^*$.

III. RESULTS

A. Monte Carlo simulation

In this work we investigate the effect of disorder on the fluid-fluid binodals for $q = 0.8$. We perform simulations in the absence of the porous matrix — our results are consistent with those of Refs. [32, 33] — and for two values of f , $f = 0.4$ and $f = 0.7$ [note that $\hat{c}(f = 0.7) \approx 2\hat{c}(f = 0.4)$], in cubic boxes L^3 with $L/R_c = 16$ and 20 . In order to obtain quenched averages we consider 200-400 matrix realizations for each f and R_{dis} .

For each value of f we consider a few values of R_{dis}/R_c . For $f = 0.4$ we present results for $R_{\text{dis}}/R_c = 0.2, 0.6, 1.0$ ($f_{\text{pol}} = 0.26, 0.29$, and 0.31 , respectively), while for $f = 0.7$, we use $R_{\text{dis}}/R_c = 0.2$ and 1.0 ($f_{\text{pol}} = 0.50$ and 0.57 , respectively). It should be noted that we are limited by computer power in further decreasing or increasing the ratio R_{dis}/R_c . Indeed, if we further decrease the ratio, the disorder density increases, see Table I, and so does the number of matrix particles and the computational work. On other hand, if we increase R_{dis}/R_c beyond 1, we should consider quite large systems in order to avoid large size effects, which is unfeasible with our present computer power.

In order to determine the coexistence curves we perform a grand-canonical simulation. The grand partition sum for each disorder realization is

$$\Xi(V, z_p, z_c) = \sum_{N_p, N_c} z_p^{N_p} z_c^{N_c} Q(V, N_p, N_c), \quad (7)$$

where $Q(V, N_p, N_c)$ is the configurational partition function of a system of N_p polymers and N_c colloids in a volume V , and z_p and z_c are the corresponding fugacities. In Eq. (7) we normalize $Q(V, N_p, N_c)$ so that $Q(V, 1, 0) = Q(V, 0, 1) = V$, hence z_p and z_c are dimensionful parameters. We quote our results in terms of the dimensionless combinations $z_c R_c^3$ and

$$\eta_p^r = \frac{4\pi}{3} z_p R_p^3. \quad (8)$$

The quantity η_p^r represents the polymer reservoir packing fraction.

In the presence of a first-order transition, standard local algorithms are unable to sample correctly both phases in the simulation. We therefore combine the grand-canonical algorithm with the umbrella sampling and the simulated-tempering method [55, 56], as discussed in App. A. Insertions and deletions of colloids and polymers are performed by using the cluster moves introduced by Vink and Horbach [31, 57].

B. Quenched coexistence curve

The main purpose of this work is the determination of the disorder-averaged coexistence curve. In order to define it precisely, let us define the disorder-averaged colloid and polymer numbers

$$\begin{aligned} N_{c,\text{av}}(V, z_p, z_c) &= z_c \frac{\partial}{\partial z_c} [\ln \Xi(V, z_p, z_c)], \\ N_{p,\text{av}}(V, z_p, z_c) &= z_p \frac{\partial}{\partial z_p} [\ln \Xi(V, z_p, z_c)], \end{aligned} \quad (9)$$

where $[\cdot]$ indicates the average over the matrix realizations. In the presence of first-order transitions, there is a line $z_c = z_c^*(z_p)$ in the (z_p, z_c) plane where these two functions become discontinuous in the infinite-volume limit. In other words, for $z_p > z_{p,\text{crit}}$ we have

$$\begin{aligned} \lim_{\epsilon \rightarrow 0^+} \lim_{V \rightarrow \infty} N_{c,\text{av}}(V, z_p, z_c^*(z_p) + \epsilon)/V &= c_{c,\text{liq}}, \\ \lim_{\epsilon \rightarrow 0^+} \lim_{V \rightarrow \infty} N_{p,\text{av}}(V, z_p, z_c^*(z_p) + \epsilon)/V &= c_{p,\text{liq}}, \\ \lim_{\epsilon \rightarrow 0^+} \lim_{V \rightarrow \infty} N_{c,\text{av}}(V, z_p, z_c^*(z_p) - \epsilon)/V &= c_{c,\text{gas}}, \\ \lim_{\epsilon \rightarrow 0^+} \lim_{V \rightarrow \infty} N_{p,\text{av}}(V, z_p, z_c^*(z_p) - \epsilon)/V &= c_{p,\text{gas}}. \end{aligned} \quad (10)$$

The pair $c_{p,\text{liq}}, c_{c,\text{liq}}$ gives the polymer and colloid concentrations in the colloid-liquid phase at coexistence, while $c_{p,\text{gas}}$ and $c_{c,\text{gas}}$ correspond to the colloid-gas polymer-rich phase.

In the MC simulations the position of the demixing curve can be determined by studying the disorder averaged histograms of N_c and N_p , which are defined as

$$h_{c,\text{ave}}(N_{c,0}, z_p, z_c) \equiv \left[\langle \delta(N_c, N_{c,0}) \rangle_{GC, z_p, z_c} \right], \quad (11)$$

$$h_{p,\text{ave}}(N_{p,0}, z_p, z_c) \equiv \left[\langle \delta(N_p, N_{p,0}) \rangle_{GC, z_p, z_c} \right], \quad (12)$$

where $\delta(x, y)$ is the Kronecker's delta [$\delta(x, x) = 1$, $\delta(x, y) = 0$ for $x \neq y$] and $\langle \cdot \rangle_{GC, z_p, z_c}$ is the grand-canonical ensemble average. In the two-phase region the histograms show a double-peak structure. In order to obtain z_c^* at fixed z_p in a finite volume, several different methods can be used. We followed two different recipes, the equal-area and the equal-height methods. In the first case, we define z_c^* as the value of the colloid fugacity at which the area below the two peaks is equal. For instance, if we consider the colloid-number distribution, we first compute the position N_{min} of the minimum between the two peaks and then require z_c^* to be the value of the colloid fugacity at which

$$\sum_{N_c < N_{\text{min}}} h_{c,\text{ave}}(N_c, z_p, z_c^*) = \sum_{N_c > N_{\text{min}}} h_{c,\text{ave}}(N_c, z_p, z_c^*). \quad (13)$$

Equivalently, one can use the polymer distribution $h_{p,\text{ave}}(N_c, z_p, z_c)$. In the second method we identify z_c^* as the value of the fugacity at which the two peaks have the same height. Once z_c^* has been obtained, the colloid and polymer number at the transition are defined as the positions of the maxima of the histograms.

Since we have two different histograms to analyze, we obtain two different estimates of the colloid fugacity at coexistence: an estimate $z_c^*(c)$ is obtained from the analysis of the colloid-number histograms, while $z_c^*(p)$ is obtained from the analysis of the polymer-number histograms. For $R_{\text{dis}}/R_c = 0.2, 0.6$ the two estimates are quite close and provide consistent estimates of the colloid and polymer packing fractions at coexistence, although the equal-area method is more thermodynamically consistent. Indeed, the differences $|z_c^*(c) - z_c^*(p)|$ computed with the equal-area method are always smaller than those computed with the second prescription. For $R_{\text{dis}}/R_c = 1.0$, we have been unable to apply the area method. The difficulties can be understood by looking at Fig. 2, where we report the colloid histograms for $f = 0.7$ and for the largest value of z_p we consider, $\eta_p^r \approx 1.82$ ($z_p R_c^3 = 0.85$). While the colloid-liquid peak is quite narrow, the colloid-gas peak is very broad and therefore condition (13) is satisfied only when the colloid-gas peak is barely visible. However, in this case the definition of N_{min} is ambiguous and thus z_c^* is determined with large uncertainty. In some cases, it is even impossible to satisfy the equal-area condition. Thus, for $R_{\text{dis}}/R_c = 1.0$ we only use the equal-height method. Note that the two methods should give identical results in the infinite-volume limit. Hence, the difficulties we observe indicate that for this value of the parameters finite-size effects are important. The analyses reported in the following sections confirm these findings. It is interesting to note that, at variance with what happens in the bulk, in the presence of randomness the order parameter distribution shows two well-separated nonoverlapping peaks even at the critical point (see Refs. [46, 47] for a discussion in the present context). Thus, it is also possible that the difficulties we observe for some values of the parameters are related to the fact that they belong to the one-phase region, even if the finite-size colloid and polymer histograms are bimodal.

To give an idea of the performance of the two methods, we report the results for $f = 0.4$, $R_{\text{dis}}/R_c = 0.6$, $\eta_p^r \approx 1.24$ ($z_p R_c^3 = 0.58$), and $L/R_c = 16$, see Fig. 3. The equal-area method gives

$$z_c^* R_c^3 \approx 130.2 \quad \eta_{c,\text{gas}} \approx 0.041 \quad \eta_{c,\text{liq}} \approx 0.294, \quad (14)$$

from the analysis of the colloid distribution. The analysis of the polymer distribution gives

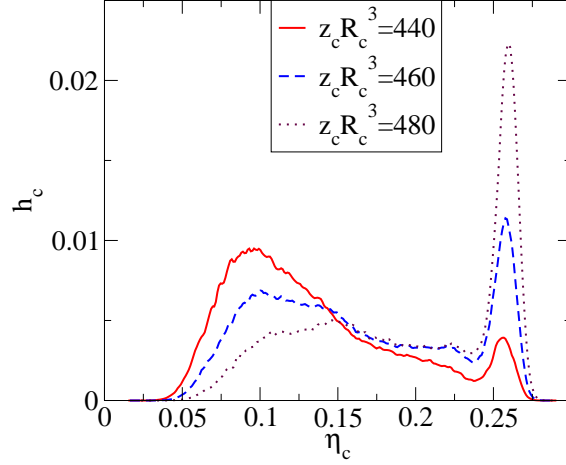


FIG. 2: Colloid histogram $h_{c,ave}$ for $L/R_c = 16$, $f = 0.7$, $R_{dis}/R_c = 1.0$, $\eta_r^r \approx 1.82$ ($z_p R_c^3 = 0.85$), and some values of z_c close to z_c^* .

the same estimate of z_c^* (we have data for several values of z_c with step $\Delta z_c = 0.1$). If we apply instead the equal-height method we obtain $z_c^*(c)R_c^3 \approx 129.3$ and $z_c^*(p)R_c^3 \approx 127.5$ from the two distributions. The colloid packing fractions at coexistence are therefore

$$\begin{aligned} z_c^*(c)R_c^3 = 129.3 & & \eta_{c,gas} \approx 0.039 & & \eta_{c,liq} \approx 0.294, \\ z_c^*(p)R_c^3 = 127.5 & & \eta_{c,gas} \approx 0.038 & & \eta_{c,liq} \approx 0.292. \end{aligned} \quad (15)$$

The results are very close with each other and consistent with those reported in Eq. (14). Similar conclusions are obtained for the polymer packing fractions at coexistence. For $f = 0.7$, $R_{dis}/R_c = 1.0$, $\eta_r^p \approx 1.82$ ($z_p R_c^3 = 0.85$), and $L/R_c = 16$, the case reported in Fig. 2, we obtain $z_c^*(c)R_c^3 \approx 454$ and $z_c^*(p)R_c^3 \approx 440$ from the two distributions (equal-height method). At coexistence we find then

$$\begin{aligned} z_c^*(c)R_c^3 = 454 & & \eta_{c,gas} \approx 0.096 & & \eta_{c,liq} \approx 0.257, \\ z_c^*(p)R_c^3 = 440 & & \eta_{c,gas} \approx 0.100 & & \eta_{c,liq} \approx 0.258. \end{aligned} \quad (16)$$

Even though the estimates of the coexistence colloid fugacity differ somewhat, the two estimates of the colloid packing fractions at coexistence are quite close.

C. Sample-to-sample fluctuations

It is interesting to understand how the results obtained from the sample average compare with those that would be obtained by determining the coexisting phases for each disorder

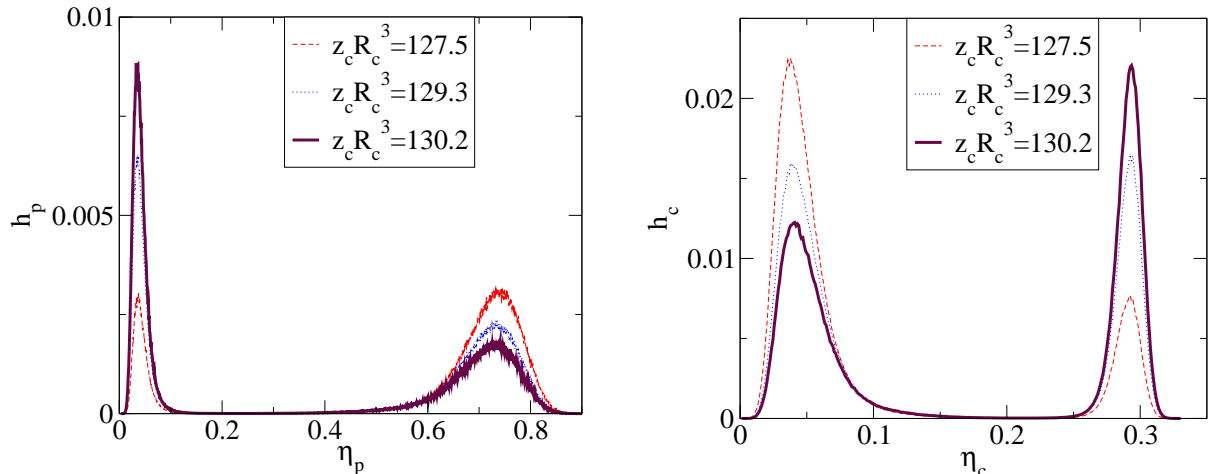


FIG. 3: Polymer histogram $h_{p,ave}$ and colloid histogram $h_{c,ave}$ for $L = 16R_c$, $f = 0.4$, $R_{dis}/R_c = 0.6$, $\eta_p^r \approx 1.24$ ($z_p R_c^3 = 0.58$), and several fugacities $z_c R_c^3$. The thicker curve corresponds to the coexistence fugacity obtained by using the equal-area prescription ($z_c^* R_c^3 = 130.2$), while the other two curves correspond to the estimates $z_c^*(c) R_c^3 = 129.3$ and $z_c^*(p) R_c^3 = 127.5$ obtained by using the equal-height method.

realization. In Fig 4 we report the distributions of the colloid and polymer packing fractions at coexistence computed from each disorder configuration. The distributions of the packing fractions corresponding to the colloid-liquid phase are very narrow and are centered at the value obtained from the analysis of the average distributions. On the other hand, the distributions for the colloid-gas phase are broad, especially for $R_{dis}/R_c = 0.6$ and 1. Since the broadness of the distribution is a finite-size effect — we expect the width of the distributions to scale as $1/\sqrt{L}$ as $L \rightarrow \infty$ — this is an indication that we should expect some finite-size dependence on our determination of the colloid-gas branch of the coexistence curves. The results reported in the next section confirm these expectations.

Finally, we also report the distributions for the case $f = 0.7$, $R_{dis}/R_c = 1$, $\eta_p^r \approx 1.82$ ($z_p R_c^3 = 0.85$) (the average colloid-number histograms are reported in Fig. 2), for which we have been unable to determine the coexistence fugacity using the equal-area method. The distribution of the colloid and polymer packing fractions at coexistence are reported in Fig. 5 and clearly explain the origin of the difficulties. The position of the colloid-gas branch varies significantly from sample to sample. We are thus far from the infinite-volume limit, since in this limit sample fluctuations are expected to disappear except close to the critical

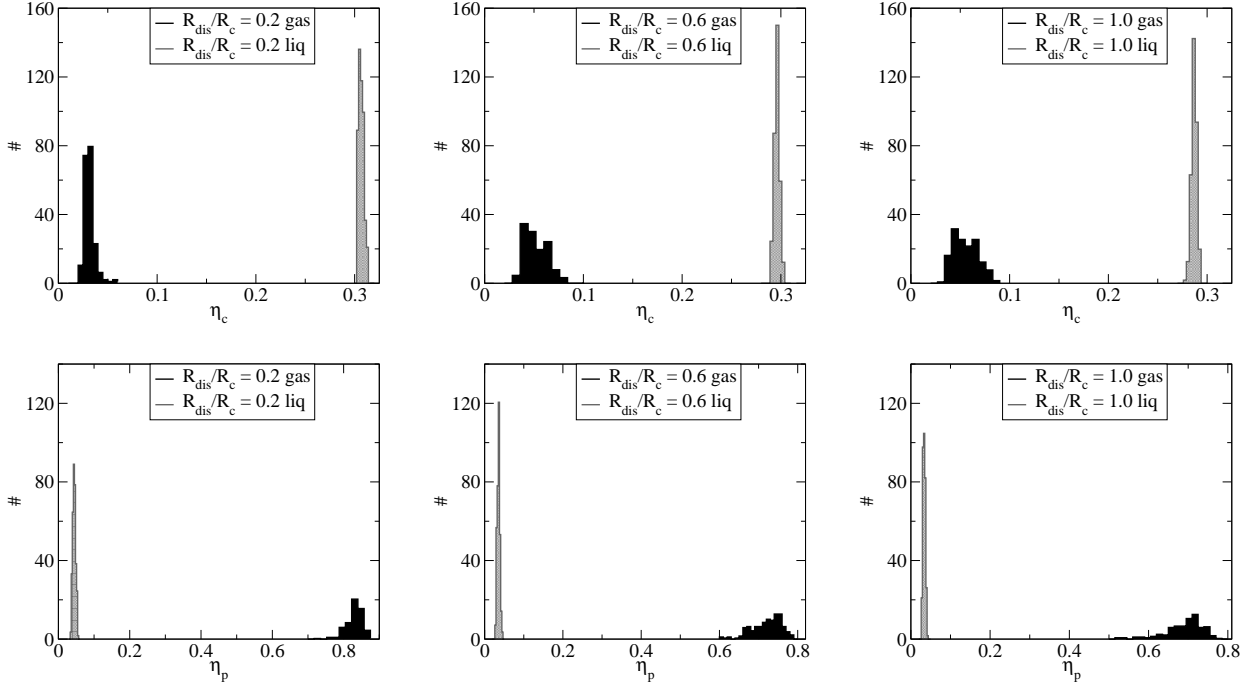


FIG. 4: (Color online) Distribution of the coexisting colloid (top) and polymer (bottom) packing fractions for $\eta_p^r \approx 1.24$ ($z_p R_c^3 = 0.58$), $f = 0.4$ and three different values of R_{dis}/R_c : 0.2, 0.6, 1.0. The colloid-gas phase data are reported in black, while the colloid-liquid phase data are reported in gray. Data from simulations with $L/R_c = 16$.

point. These results provide again evidence that size effects are large for these values of the parameters.

D. Finite-size effects

The analyses presented above show that size effects may still be relevant for the data with $L/R_c = 16$. They appear to increase with increasing f and/or R_{dis}/R_c and should be particularly large for $f = 0.7$ and $R_{\text{dis}}/R_c = 1.0$. To investigate size effects we have performed additional simulations with $L/R_c = 20$. In Fig. 6 we compare the results for the coexistence curve obtained by using these two different box sizes. We report results both in terms of η_c and η_p and also in the reservoir representation (see insets) in terms of η_c and η_p^r .

On top we show the results for $f = 0.4$. Corrections here appear to be under control: the

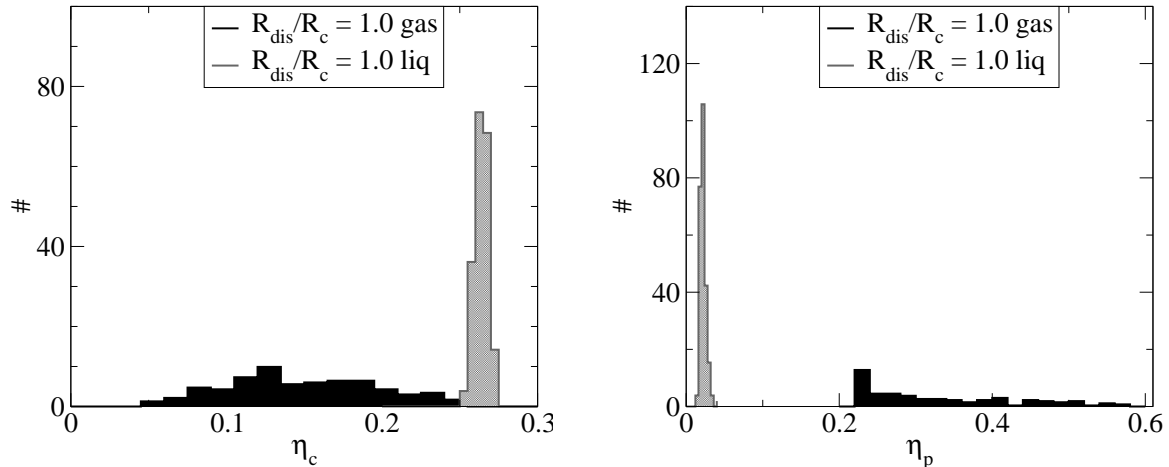


FIG. 5: Distribution of the coexisting colloid (left) and polymer (right) packing fraction for $\eta_p^r \approx 1.82$ ($z_p R_c^3 = 0.85$), $f = 0.7$ and $R_{\text{dis}}/R_c = 1$. The colloid-gas phase data are reported in black, while the colloid-liquid phase data are reported in gray. Data from simulations with $L/R_c = 16$.

plots in the terms of η_c and η_p show a small size dependence, while those in the reservoir representation appear to be reliable except close to the critical point, which is not unexpected since size corrections are large in a neighborhood of a second-order phase transition. For $f = 0.7$, the colloid-liquid branch is determined quite reliably. On the other hand, the colloid-gas phase boundary varies significantly when L changes, especially for the case $R_{\text{dis}}/R_c = 1.0$. This is not unexpected, given the results shown in the previous sections. Indeed, in all cases the polymer and colloid histograms are characterized by very narrow colloid-liquid peaks whose positions have a tiny dependence on the fugacity z_c , so that, even if z_c^* is not precisely determined, the determined values $\eta_{c,\text{liq}}$ and $\eta_{p,\text{liq}}$ are quite reliable. In the colloid-gas phase the distributions are instead very broad, a clear indication that we are far from the infinite-volume limit. As we have already remarked, it is also possible that, for some values of the parameters, the system is in the one-phase region, even if the finite-size data show double peaks.

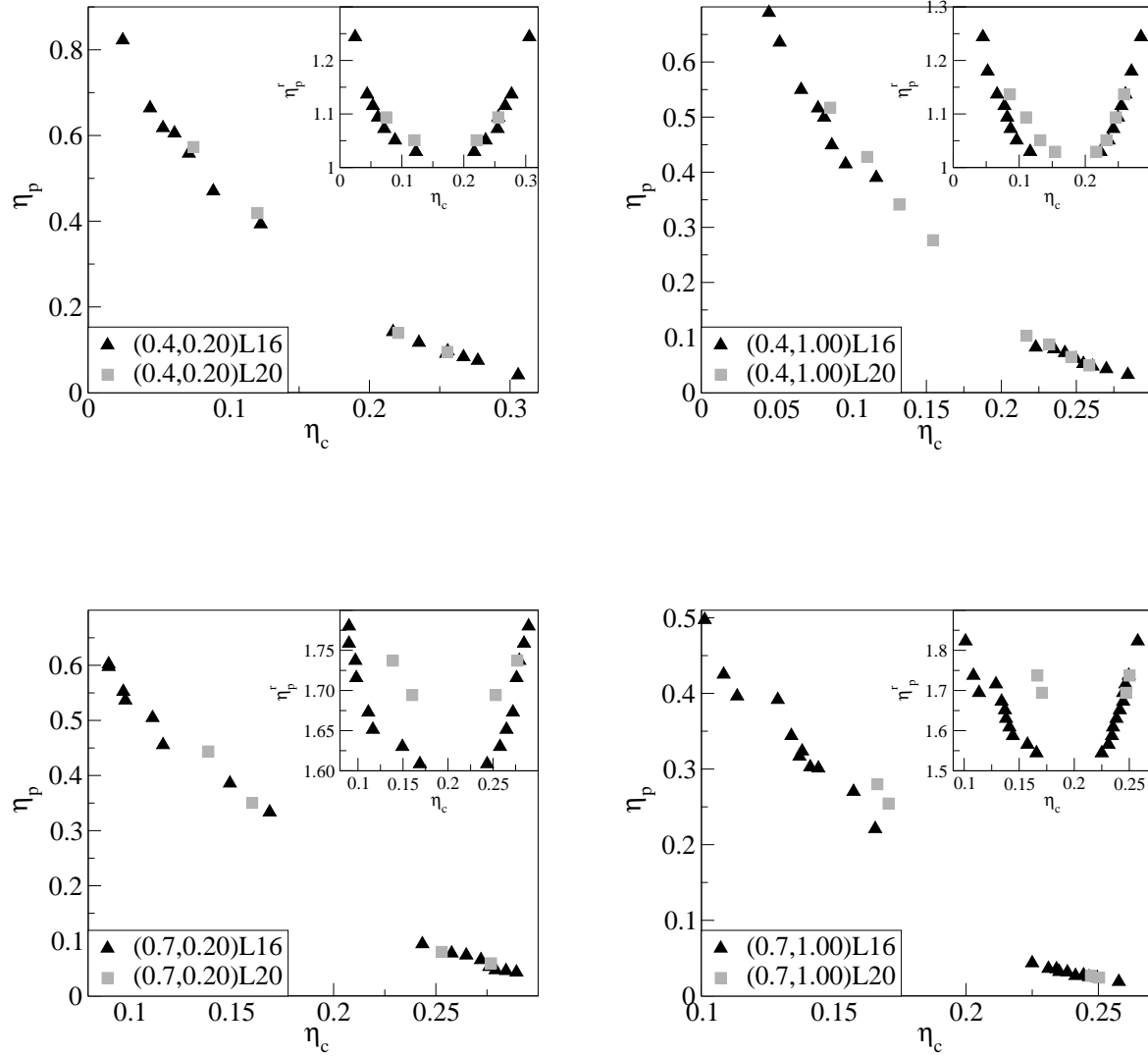


FIG. 6: Fluid-fluid binodal curves for $f = 0.4$, $R_{\text{dis}}/R_c = 0.2$ (top left), $f = 0.4$, $R_{\text{dis}}/R_c = 1.0$ (top right), $f = 0.7$, $R_{\text{dis}}/R_c = 0.2$ (bottom left), $f = 0.7$, $R_{\text{dis}}/R_c = 1.0$ (bottom right). We report the results for $L = 16R_c$ and $L = 20R_c$ in the η_c, η_p plane and (inset) in the reservoir representation η_c, η_p^r .

E. Demixing curves in the reservoir representation

The estimates of z_c^* [we report the average of $z_c^*(c)$ and $z_c^*(p)$] as a function of η_p^r for $L/R_c = 16$ are reported in Fig. 7. In order to compare our results with those of Ref. [45], we also report the estimates of the polymer reservoir packing fraction η_p^{r*} at coexistence in

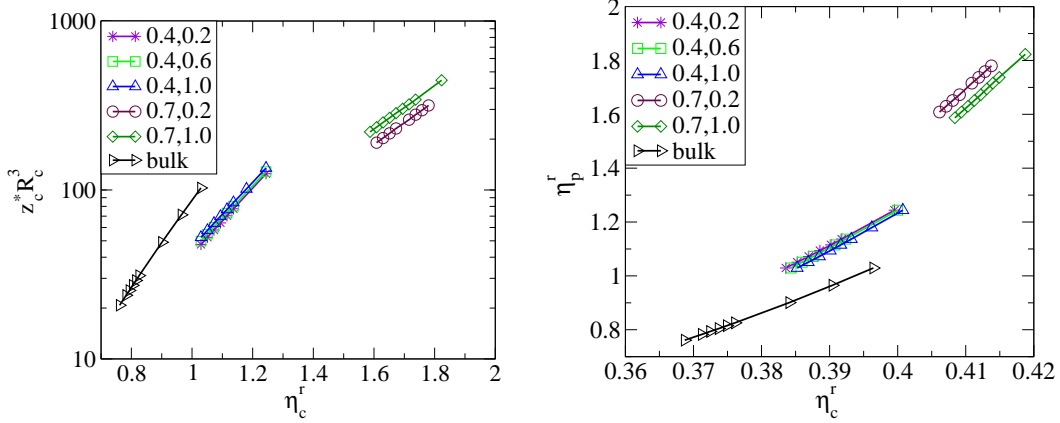


FIG. 7: Estimates of $z_c^* R_c^3$ as a function of the polymer reservoir packing fraction η_p^r (left) and of η_p^{r*} at coexistence in terms of the colloid reservoir packing fraction η_c^r (right). Results for $L/R_c = 16$. In the legend the first number corresponds to f , while the second one gives the ratio R_{dis}/R_c .

terms of the colloid reservoir packing fraction η_c^r [58]. Note that, on a logarithmic scale, the values $z_c^* R_c^3$ for each f and R_{dis}/R_c lie quite precisely on a straight line, indicating that the colloid chemical potential at coexistence is well approximated by a linear function in η_p^r . Moreover, the position of the demixing curve depends essentially only on f . The ratio R_{dis}/R_c , hence the topological structure of the matrix, does not change significantly the coexistence curve. We have not performed a careful finite-size scaling analysis close to the critical point (a detailed discussion of the methods appropriate for random-field Ising critical points is reported in Refs. [47, 59, 60]) and thus we are not able to estimate $\eta_{p,\text{crit}}^r$ and $\eta_{c,\text{crit}}^r$ precisely. We only note that for $L/R_c = 16$ and $L/R_c = 20$ double peaks are observed only for $\eta_p^r \gtrsim 1.00, 1.03$ for all three values of R_{dis}/R_c . We can thus set the lower bounds $\eta_{p,\text{crit}}^r \gtrsim 1.03$ and $\eta_{c,\text{crit}}^r \gtrsim 0.38$. For $f = 0.7$ size effects are significantly larger than for $f = 0.4$, but we can still obtain the bounds $\eta_{p,\text{crit}}^r \gtrsim 1.6, \eta_{c,\text{crit}}^r \gtrsim 0.405$.

We can use our results to understand qualitatively the behavior of a bulk colloid-polymer mixture in chemical equilibrium with the same dispersion adsorbed in a porous matrix. The main question is whether one can observe different phases in the bulk and in the matrix. If we use η_c^r as control parameter, we see that for $\eta_c^r < \eta_{c,\text{crit},\text{bulk}}^r \approx 0.37$ there is no transition, neither in the bulk nor in the matrix. If η_c^r is larger, one may have a transition in the bulk and no transition in the matrix, given that $\eta_{c,\text{crit}}^r$ increases with f . For instance, for $f = 0.4$ and $0.37 \lesssim \eta_c^r \lesssim 0.385$ we only observe phase separation in the bulk. If we increase

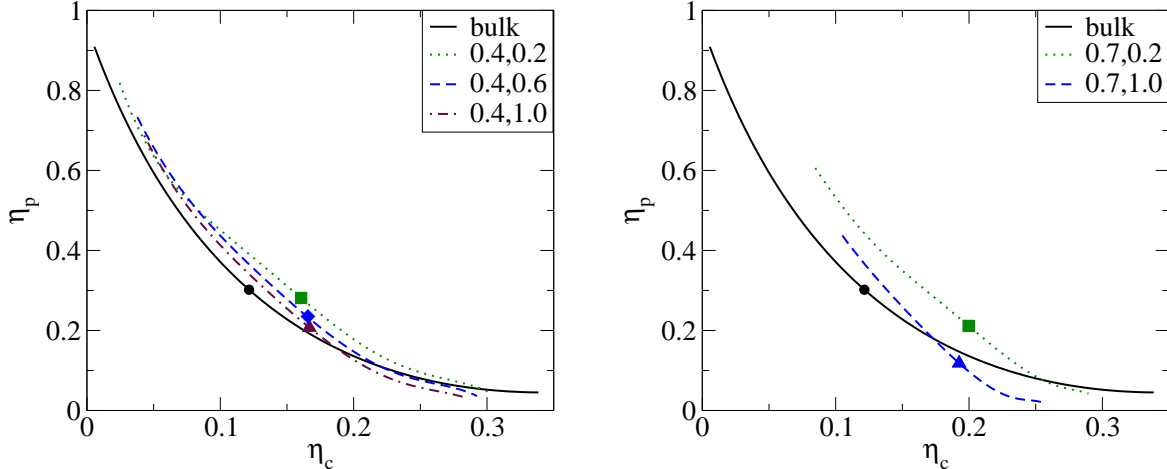


FIG. 8: Binodal curves (obtained by interpolating the data reported in Fig. 6) for $f = 0.40$ (left) and $f = 0.70$ (right). In both plots we also report the bulk binodal curve and the effective critical points. In the legend the first number corresponds to f , while the second one gives the ratio R_{dis}/R_c . Simulations in a box of size $L = 16R_c$.

further η_c^r ($\eta_c^r \gtrsim 0.385$ for $f = 0.4$) the behavior is more complex, since phase separation occurs both in the bulk and in the matrix. For small η_p^r the mixture is in the colloid-liquid phase both in the bulk and in the matrix. If η_p^r is increased, that is polymers are added, the bulk coexistence curve is reached, see Fig. 7. Above the demixing line, one observes two different phases: in the bulk the system is in the colloid-gas phase, while in the matrix a colloid-liquid phase occurs. Thus, the presence of the matrix may induce, for certain values of the parameters, a capillary condensation of the colloids. Finally, for large η_p^r above the matrix coexistence curve, a colloid-gas phase occurs both in the bulk and in the matrix.

F. Binodals in the system representation

In Fig. 8 we report the results for the binodals (we interpolate the MC data for $L/R_c = 16$) as a function of η_c and η_p . For $f = 0.4$ they are quite close to the bulk binodal curve and show only a tiny dependence on the ratio R_{dis}/R_c . In the figure we also report an estimate of the critical point obtained by determining the intersection of the diameter with the interpolation of the coexistence data. This provides a very rough estimate of the critical parameters, which can only be accurately determined by performing a careful finite-size scaling analysis. In

the bulk the analysis of the results with $L/R_c = 16$ gives $\eta_{c,\text{crit}} \approx 0.12$, $\eta_{p,\text{crit}} \approx 0.31$, which should be compared with the precise determination [31, 32]

$$\eta_{c,\text{crit}} = 0.1340(2), \quad \eta_{p,\text{crit}} = 0.3562(6). \quad (17)$$

Apparently our simple extrapolation underestimates $\eta_{c,\text{crit}}$ by 10% and $\eta_{p,\text{crit}}$ by 15%, which we can take as indications of the systematic error. If we perform the same analysis for $f = 0.4$ we obtain $\eta_{c,\text{crit}} \approx 0.17$ for all values of R_{dis}/R_c : the colloid packing fraction at criticality is essentially independent of the matrix topology and increases with increasing f . As for the polymer packing fraction, the dependence on the size ratio R_{dis}/R_c is somewhat larger. The value $\eta_{p,\text{crit}}$ decreases with increasing R_{dis}/R_c and varies between 0.23 and 0.29. If we assume that the results for $L/R_c = 16$ underestimate the correct, infinite-volume results by 10% and 15% as they do in the bulk, we would guess $\eta_{c,\text{crit}} \approx 0.19$ and $0.27 \lesssim \eta_{p,\text{crit}} \lesssim 0.34$.

As we have already stated our results for $f = 0.7$ are only reliable in the colloid-liquid phase. In this regime the binodal curve depends somewhat on R_{dis}/R_c : for $R_{\text{dis}}/R_c = 0.2$ it is close to the bulk curve, while for $R_{\text{dis}}/R_c = 1$ it is significantly below it. The critical point position is consistent with what was observed for $f = 0.4$: $\eta_{c,\text{crit}}$ shows little dependence on R_{dis}/R_c , while $\eta_{p,\text{crit}}$ decreases with increasing R_{dis}/R_c .

We can compare our results with those obtained in Refs. [45, 48]. By using density-functional methods, Ref. [45] studied the model with $R_{\text{dis}}/R_c = 1$ at the slightly lower value of f , $f = 0.37$ (corresponding to $\eta_{\text{dis}} = 0.05$), and several values of q , $q = 0.3, 0.6, 1.0$ (none of them agrees unfortunately with ours). Their results are not consistent with ours. They find that in all cases the binodal curve in the presence of the matrix is below that in the bulk, while here we find the opposite except deep in the colloid-liquid region, i.e. for $\eta_c \gtrsim 0.20$. Moreover, they find that $\eta_{c,\text{crit}}$ decreases with increasing f in all cases, which is again in contrast with our results. On the other hand we are fully consistent with the results of Ref. [48], which study the model for $R_{\text{dis}}/R_c = 1$, $f = 0.37$ ($\eta_{\text{dis}} = 0.05$), and $q = 0.8$. For the critical point they obtain $\eta_{c,\text{crit}} = 0.192$ and $\eta_{p,\text{crit}} = 0.292$, confirming that $\eta_{c,\text{crit}}$ increases in the presence of disorder. From a quantitative point of view, their critical-point estimates are fully consistent with ours. In particular, the naive extrapolation we have performed above apparently estimates correctly the critical-point position at the 5% level.

IV. CONCLUSIONS

In this paper we determine the fluid-fluid demixing curves for the AO model in a colloidal matrix for $q = 0.8$ and several values of R_{dis}/R_c and f (equivalently, of the disorder concentration c_{dis}). This study should provide quantitative informations on the phase behavior of a polymer-colloid mixture in a porous material close to the θ point. Our main results are the following:

- Disorder is specified by two parameters: the disorder packing fraction η_{dis} and the ratio R_{dis}/R_c . At least for $R_{\text{dis}}/R_c \leq 1$, the parameter range we consider, most of the disorder dependence of the results can be parametrized by using a single parameter, the effective matrix filled-space ratio f , which gives the volume fraction unavailable to the colloids. In the z_p, z_c plane (or equivalently in terms of the reservoir packing fractions η_c^r and η_p^r) the coexistence curve depends essentially only on f .
- It is possible to observe capillary condensation of the colloids. For certain values of the parameters a colloid-gas bulk phase is in equilibrium with a colloid-liquid phase in the matrix.
- At least for $f \lesssim 0.4$ the binodal curves expressed in terms of the packing fractions (system representation) show a relatively small dependence on disorder. The critical point instead changes significantly. The critical colloid packing fraction $\eta_{c,\text{crit}}$ is, to a large extent, only a function of f and it increases as f increases. The critical polymer packing fraction $\eta_{p,\text{crit}}$ depends instead both on f and R_{dis}/R_c . At fixed f it decreases as R_{dis}/R_c increases.

The authors gratefully acknowledge extensive discussions with Ettore Vicari. The MC simulations were performed at the INFN Pisa GRID DATA center and on the INFN cluster CSN4.

Appendix A: Monte Carlo simulations: some technical details

We have performed simulations in the grand-canonical (GC) ensemble, which physically describes a system adsorbed in a colloid matrix in chemical equilibrium with a reservoir of

pure polymers and a reservoir of pure noninteracting colloids. The basic parameters are the colloid and polymer fugacities z_c and z_p . In the bulk the partition function is

$$\Xi(V, z_p, z_c) = \sum_{N_p, N_c} z_p^{N_p} z_c^{N_c} Q(V, N_p, N_c), \quad (\text{A1})$$

where $Q(V, N_p, N_c)$ is the configurational partition function of a system of N_p polymers and N_c colloids in a volume V . We drop the irrelevant thermal length so that $Q(V, 1, 0) = Q(V, 0, 1) = V$. In the presence of first-order transitions it is quite difficult to sample correctly the GC distribution. To bypass the difficulties we use the umbrella-sampling (sometimes also called multicanonical) method [55]. Instead of generating configurations with the GC weight, we use an umbrella distribution

$$\frac{1}{\pi(N_c)} z_p^{N_p} z_c^{N_c} e^{-\beta H}, \quad (\text{A2})$$

with a properly chosen $\pi(N_c)$ which is defined below. If $\langle \cdot \rangle_{GC}$ and $\langle \cdot \rangle_\pi$ are the averages with respect to the GC distribution and to the distribution (A2), respectively, we have

$$\langle O(N_c, N_p) \rangle_{GC} = \frac{\langle \pi(N_c) O(N_c, N_p) \rangle_\pi}{\langle \pi(N_c) \rangle_\pi}. \quad (\text{A3})$$

This relation allows us to obtain GC averages from simulations using the distribution (A2). The function $\pi(N_c)$ must be chosen so that in the simulation the system can move easily between the two phases. Consider the histogram of N_c in the GC distribution, i.e.

$$h(N_{c,0}) = \langle \delta(N_c, N_{c,0}) \rangle_{GC}, \quad (\text{A4})$$

where $\delta(x, y)$ is Kronecker's delta. Assume that the system is close to phase separation so that $h(N_c)$ has two peaks at $N_{c,\min}$ (colloid-gas phase) and $N_{c,\max}$ (colloid-liquid phase). The optimal choice is then

$$\begin{aligned} \pi(N) &= ah(N_{c,\min}) & N &\leq N_{c,\min}, \\ \pi(N) &= ah(N) & N_{c,\min} &\leq N \leq N_{c,\max}, \\ \pi(N) &= ah(N_{c,\max}) & N &\geq N_{c,\max}, \end{aligned} \quad (\text{A5})$$

where a is an irrelevant constant. Indeed, if $N_{c,\min} \leq N_c \leq N_{c,\max}$, the observed histogram in the umbrella distribution is flat, i.e. independent of N_c . Hence, the system can move freely between the two phases, allowing a precise determination of any required thermodynamic property.

In order to determine the colloid fugacity z_c^* at coexistence for a given value of the polymer fugacity z_p , we consider N_m colloid fugacities $\{z_{c,m}\}$, such that for $z_{c,1}$ (z_{c,N_m}) the system is in the colloid-gas (colloid-liquid) phase. Then, we determine the umbrella functions $\pi_m(N_c)$ iteratively. First, we perform a short hysteresis cycle in which we perform N_{therm} GC iterations at $z_c = z_{c,1}$, then at $z_{c,2}$, and so on, up to z_{c,N_m} ; then we decrease z_c till we reach again $z_{c,1}$. If $h_m^{(1),+}(N_c)$ and $h_m^{(1),-}(N_c)$ are the histograms obtained at $z = z_m$ (the $+$ refers to the distribution obtained while increasing z_c and the $-$ to that obtained while decreasing the fugacity), we set $h_m^{(1)}(N_c) = h_m^{(1),+}(N_c) + h_m^{(1),-}(N_c)$ and

$$\begin{aligned} \pi_m^{(1)}(N_c) &= h_m^{(1)}(N_c)/M && \text{if } h_m^{(1)}(N_c) \geq M, \\ \pi_m^{(1)}(N_c) &= 1 && \text{if } h_m^{(1)}(N_c) \leq M, \end{aligned} \quad (\text{A6})$$

where $M \equiv \max_{N_c}[h_m^{(1)}(N_c)]/10$. Then, we repeat again the same hysteresis cycle several times. At iteration k , for each $z_{c,m}$ we perform the simulation using the distribution (A2) with $\pi = \pi_m^{(k-1)}$. Then, we set

$$\begin{aligned} \pi_m^{(k)}(N_c) &= \pi_m^{(k-1)}(N_c)h_m^{(k)}(N_c)/M && \text{if } h_m^{(k)}(N_c) \geq M, \\ \pi_m^{(k)}(N_c) &= \pi_m^{(k-1)}(N_c) && \text{if } h_m^{(k)}(N_c) \leq M, \end{aligned} \quad (\text{A7})$$

where $M \equiv \max_{N_c}[h_m^{(k)}(N_c)]/10$. We stop when we observe that, for at least some values of m , $h_m^{(k),+}(N_c)$ and $h_m^{(k),-}(N_c)$ are nonvanishing in an interval of values of N_c that extends between the two phases.

Once we have a reasonable estimate of the functions $\pi_m(N_c)$, we could just perform an extensive simulation at single value of $z_{c,m}$, (an optimal choice would be to take the value for which $\pi_m(N_c)$ is clearly bimodal). Data for different values of z_c could just be obtained by standard reweighting techniques. However, we have found more convenient, to use all information we have collected and simulate all systems together, using the simulated-tempering method [56]. Note that, in the standard implementation of the method, one should be careful that the fugacities $z_{c,m}$ are such that the colloid-number distributions overlap; otherwise, no fugacity swap is accepted. In our case, since we use umbrella distributions, the overlap condition is always verified, and thus the number N_m of needed systems is always small. Typically we take $N_m = 10$. If

$$\Xi_{\pi_m}(V, z_p, z_{c,m}) = \sum_{N_p, N_c} \frac{z_p^{N_p} z_{c,m}^{N_c}}{\pi_m(N_c)} Q(V, N_p, N_c), \quad (\text{A8})$$

we consider the extended partition function

$$\Xi^{ST} = \sum_m f_m \Xi_{\pi_m}(V, z_p, z_{c,m}). \quad (\text{A9})$$

The constants f_m are chosen so that all terms in the sum are approximately equal. If we require

$$f_m \Xi_{\pi_m}(V, z_p, z_{c,m}) = f_{m-1} \Xi_{\pi_{m-1}}(V, z_p, z_{c,m-1}), \quad (\text{A10})$$

we obtain

$$\frac{f_m}{f_{m-1}} = R_m \quad \frac{f_{m-1}}{f_m} = S_m, \quad (\text{A11})$$

with

$$R_m \equiv \left\langle \left(\frac{z_{c,m-1}}{z_{c,m}} \right)^{N_c} \frac{\pi_m(N_c)}{\pi_{m-1}(N_c)} \right\rangle_{\pi,m}, \quad (\text{A12})$$

$$S_m \equiv \left\langle \left(\frac{z_{c,m}}{z_{c,m-1}} \right)^{N_c} \frac{\pi_{m-1}(N_c)}{\pi_m(N_c)} \right\rangle_{\pi,m-1}, \quad (\text{A13})$$

where $\langle \cdot \rangle_{\pi,m}$ indicates the mean value with respect to the umbrella distribution (A2) with $z_c = z_{c,m}$, $\pi = \pi_m$. Combining these expressions we define the ratios as

$$\frac{f_m}{f_{m-1}} = \sqrt{R_m/S_m}. \quad (\text{A14})$$

The constants R_m and S_m are determined together with the umbrella sampling functions π_m . Then, we set $f_1 = 1$ and use Eq. (A14) to determine the constants f_m , $m \geq 2$.

In the matrix case, the GC partition function is still given by Eq. (A1), with the only difference that one should take into account the interactions between the freely moving particles and the matrix. Since the GC partition function depends on the matrix, also the functions π_m and the constants f_m are matrix dependent. Thus, we recompute them when we restart the simulation with the different matrix.

In the MC simulations we take $N_m \approx 10$. One MC iteration consists in 3 fugacity swaps and 1000-5000 GC moves in which colloids and polymers are inserted or removed. For this purpose we use the cluster move discussed in Ref. [57] together with standard moves in which a single polymer is removed or inserted. For each disorder instance, we perform N_{ini} iterations to determine the umbrella functions and then N_{iter} iterations to measure several histograms. Typically, N_{ini} varies between $5000N_m$ and $20000N_m$, while N_{iter} is of the order of $20000N_m$.

In the simulation we determine the colloid and polymer histograms for a large number (typically 100) of colloid fugacities $z_{c,r}$. They are obtained by measuring, for each matrix realization α , the reweighted histograms $p_c(\alpha, z_{c,r}, N_{c,0})$ and $p_p(\alpha, z_{c,r}, N_{p,0})$:

$$p_c(\alpha, z_{c,r}, z_{c,m}, N_{c,0}) = \sum_i \left(\frac{z_{c,r}}{z_{c,m}} \right)^{N_{c,i}} \pi_m(N_{c,i}) \delta(N_{c,i}, N_{c,0}) \delta(z_{c,m}, z_{c,i}), \quad (\text{A15})$$

$$p_p(\alpha, z_{c,r}, z_{c,m}, N_{p,0}) = \sum_i \left(\frac{z_{c,r}}{z_{c,m}} \right)^{N_{c,i}} \pi_m(N_{c,i}) \delta(N_{p,i}, N_{p,0}) \delta(z_{c,m}, z_{c,i}), \quad (\text{A16})$$

where i refers to the MC iteration, and $N_{p,i}$, $N_{c,i}$, $z_{c,i}$ are the number of polymers and colloids and the colloid fugacity at the i th iteration. The colloid histogram is then

$$h_{c,\text{ave}}(N_{c,0}, z_p, z_{c,r}) = \frac{1}{N_\alpha} \sum_\alpha \left[\frac{p_c(\alpha, z_{c,r}, z_{c,m}, N_{c,0})}{\sum_{N_c} p_c(\alpha, z_{c,r}, z_{c,m}, N_c)} \right], \quad (\text{A17})$$

where N_α is the number of matrix realizations. Note that we obtain a different estimate of the distributions at $z_{c,r}$ for each of the $z_{c,m}$.

As a final comment, note that our estimates (A17) are biased, since they are disorder averages of a ratio of thermal averages. This means that, if we take the limit $N_\alpha \rightarrow \infty$ at fixed N_{iter} , we obtain estimates that differ from the correct result by a term (the *bias*) of order $1/N_{\text{iter}}$. One could perform a bias correction, as discussed in Ref. [61]. However, given the small number of disorder instances, we have found that in the present case the bias correction is not relevant.

-
- [1] W. C. K. Poon, J. Phys.: Condensed Matter **14**, R859 (2002).
 - [2] M. Fuchs and K. S. Schweizer, J. Phys.: Condensed Matter **14**, R239 (2002).
 - [3] R. Tuinier, J. Rieger, and C. G. de Kruif, Adv. Colloid Interface Sci. **103**, 1 (2003).
 - [4] K. J. Mutch, J. S. van Duijneveldt, and J. Eastoe, Soft Matter **3**, 155 (2007).
 - [5] G. J. Fleer and R. Tuinier, Adv. Coll. Interface Sci. **143**, 1 (2008).
 - [6] O. Myakonkaya and J. Eastoe, Adv. Coll. Interface Sci. **149**, 39 (2009).
 - [7] T. C. Lee, J. T. Lee, D. R. Pilaski, and M. Robert, Physica A **329**, 411 (2003).
 - [8] G. A. Vliegthart, J. S. van Duijneveldt, and B. Vincent, Faraday Discuss. **123**, 65 (2003).
 - [9] S. A. Shah, Y. L. Chen, K. S. Schweizer, and C. F. Zukoski, J. Chem. Phys. **118**, 3350 (2003).
 - [10] T. Kramer, S. Scholz, M. Maskros, and K. Huber, J. Colloid Interface Sci. **279**, 447 (2004).

- [11] I. Lynch, S. Cornen, and L. Piculell, *J. Phys. Chem. B* **108**, 5443 (2004).
- [12] Y. Hennequin, M. Evens, C. M. Q. Angulo, and J. S. van Duijneveldt, *J. Chem. Phys.* **123**, 054906 (2005).
- [13] T. Kramer, R. Schweins, and K. Huber, *J. Chem. Phys.* **123**, 014903 (2005); *Macromolecules* **38**, 151 (2005); **38**, 9783 (2005).
- [14] Z. Zhang and J. S. van Duijneveldt, *Langmuir* **22**, 63 (2006).
- [15] M. Laurati, G. Petekidis, N. Koumakis, F. Cardineaux, A. B. Schofield, J. M. Brader, M. Fuchs, and S. U. Egelhaaf, *J. Chem. Phys.* **130**, 134907 (2009).
- [16] K. J. Mutch, J. S. van Duijneveldt, J. Eastoe, I. Grillo, and R. K. Heenan, *Langmuir* **25** 3944 (2009); **26**, 1630 (2010).
- [17] A. P. Gast, C. K. Hall, and W. B. Russell, *J. Colloid Interface Sci.* **96**, 251 (1983).
- [18] H. N. W. Lekkerkerker, W. C. K. Poon, P. N. Pusey, A. Stroobants, and P. B. Warren, *Europhys. Lett.* **20**, 559 (1992).
- [19] E. J. Meijer and D. Frenkel, *J. Chem. Phys.* **100**, 6873 (1994).
- [20] R. P. Sear, *Phys. Rev. E* **56**, 4463 (1997); *Phys. Rev. E* **66**, 051401 (2002).
- [21] M. Dijkstra, J. M. Brader, and R. Evans, *J. Phys.: Condensed Matter* **11**, 10079 (1999).
- [22] M. Fuchs and K. S. Schweizer, *Europhys. Lett.* **51**, 621 (2000).
- [23] M. Schmidt, H. Löwen, J. M. Brader, and R. Evans, *Phys. Rev. Lett.* **85**, 1934 (2000); *J. Phys.: Condensed Matter* **14**, 9353 (2002).
- [24] P. G. Bolhuis, A. A. Louis, and J. P. Hansen, *Phys. Rev. Lett.* **89**, 128302 (2002).
- [25] M. Dijkstra and R. van Roij, *Phys. Rev. Lett.* **89**, 208303 (2002).
- [26] J. Dzubiella, C. N. Likos, and H. Löwen, *J. Chem. Phys.* **116**, 9518 (2002).
- [27] P. G. Bolhuis, A. A. Louis, and E. J. Meijer, *Phys. Rev. Lett.* **90**, 068304 (2003).
- [28] A. Moncho-Jorda, A. A. Louis, P. G. Bolhuis, and R. Roth *J. Phys.: Condensed Matter* **48**, S3429 (2003).
- [29] R. Tuinier, *Eur. Phys. J. E* **10**, 123 (2003).
- [30] P. Paricaud, S. Varga, and G. Jackson, *J. Chem. Phys.* **118**, 8525 (2003).
- [31] R. L. C. Vink and J. Horbach, *J. Chem. Phys.* **121**, 3253 (2004).
- [32] R. L. C. Vink, J. Horbach, and K. Binder, *Phys. Rev. E* **71**, 011401 (2005).
- [33] R. L. C. Vink and M. Schmidt, *Phys. Rev. E* **71**, 051406 (2005).
- [34] R. L. C. Vink, A. Jusufi, J. Dzubiella, and C. N. Likos, *Phys. Rev. E* **72**, 030401(R) (2005).

- [35] P. Bryk, *J. Chem. Phys.* **122**, 064902 (2005).
- [36] M. Fasolo and P. Sollich, *J. Phys.: Condensed Matter* **17**, 797 (2005).
- [37] A. Pelissetto and J. P. Hansen, *Macromolecules* **39**, 9571 (2006).
- [38] C.-Y. Chou, T. T. M. Vo, A. Z. Panagiotopoulos, and M. Robert, *Physica A* **369**, 275 (2006).
- [39] G. J. Fleer and R. Tuinier, *Phys. Rev. E* **76**, 041802 (2007).
- [40] J. Zausch, P. Virnau, K. Binder, J. Horbach, R. L. C. Vink, *J. Chem. Phys.* **130**, 064906 (2009).
- [41] S. Asakura and F. Oosawa, *J. Chem. Phys.* **22**, 1255 (1954).
- [42] A. Vrij, *Pure and Appl. Chem.* **48**, 471 (1976).
- [43] This is correct only for infinite-length polymers. For finite-length chains, polymers interact weakly (as an inverse power of $\ln L$, where L is the degree of polymerization) and a proper coarse-grained description requires the introduction of an attractive pair potential and of a repulsive (needed for thermodynamic stability) three-body potential, see V. Krakoviack, J. P. Hansen, and A. A. Louis, *Phys. Rev. E* **67**, 041801 (2003); C. I. Addison, A. A. Louis, and J. P. Hansen, *J. Chem. Phys.* **121**, 612 (2004); A. Pelissetto and J. P. Hansen, *J. Chem. Phys.* **122**, 134904 (2005).
- [44] For a list of experimental studies of binary mixtures in porous materials, see the references cited in E. Schöll-Paschinger, D. Levesque, J.-J. Weis, and G. Kahl, *Phys. Rev. E* **64**, 011502 (2001).
- [45] M. Schmidt, E. Schöll-Paschinger, J. Köfinger, and G. Kahl, *J. Phys.: Condensed Matter* **14**, 12099 (2002).
- [46] R. L. C. Vink, K. Binder, and H. Löwen, *Phys. Rev. Lett.* **97**, 230603 (2006).
- [47] R. L. C. Vink, K. Binder, and H. Löwen, *J. Phys.: Condensed Matter* **20**, 404222 (2008).
- [48] G. Pellicane, R. L. C. Vink, C. Caccamo, and H. Löwen, *J. Phys.: Condensed Matter* **20**, 115101 (2008).
- [49] R. L. C. Vink, *Soft Matter* **5**, 4388 (2009).
- [50] P. G. de Gennes, *J. Phys. Chem.* **88**, 6469 (1984).
- [51] P. G. De Sanctis Lucentini and G. Pellicane, *Phys. Rev. Lett.* **101**, 246101 (2008).
- [52] T. Fischer and R. L. C. Vink, *J. Chem. Phys.* **134**, 055106 (2011).
- [53] H. Scher and R. Zallen, *J. Chem. Phys.* **53**, 3759 (1970).
- [54] W. G. Hoover and F. H. Ree, *J. Chem. Phys.* **47**, 4873 (1967).

- [55] G. M. Torrie and J. P. Valleau, *J. Comp. Phys.* **23**, 197 (1977).
- [56] E. Marinari and G. Parisi, *Europhys. Lett.* **19**, 451 (1992).
- [57] R. L. C. Vink in “Computer simulation studies in condensed matter physics XVIII,” edited by D. P. Landau, S. P. Lewis, and H. B. Schuettler (Springer, Berlin, 2004).
- [58] We use the Carnahan-Starling expression to relate the colloid reservoir packing fraction η_c^r to the fugacity z_c : $z_c R_c^3 = 3\eta_c^3 / (4\pi) \exp[f(\eta_c^r)]$ with $f(\eta) = \eta(8 - 9\eta + 3\eta^2) / (1 - \eta)^3$; see N. F. Carnahan and K. E. Starling, *J. Chem. Phys.* **51**, 635 (1969); L. L. Lee, *J. Chem. Phys.* **103**, 9388 (1995).
- [59] R. L. C. Vink, T. Fischer, and K. Binder, *Phys. Rev. E* **82**, 051134 (2010).
- [60] T. Fischer and R. L. C. Vink, *J. Phys.: Condensed Matter* **23**, 234117 (2011).
- [61] M. Hasenbusch, F. Parisen Toldin, A. Pelissetto, and E. Vicari, *J. Stat. Mech.: Theory Exp.* P02016 (2007).